



ELSEVIER

Contents lists available at SciVerse ScienceDirect

Talanta

journal homepage: www.elsevier.com/locate/talanta

Short communication

Nonenzymatic electrochemical glucose sensor based on novel Pt–Pd nanoflakes

Xiangheng Niu^a, Minbo Lan^{a,b,*}, Chen Chen^a, Hongli Zhao^{a,c,*}^a Shanghai Key Laboratory of Functional Materials Chemistry, and Research Centre of Analysis and Test, East China University of Science and Technology, Shanghai 200237, PR China^b Key Laboratory for Ultrafine Materials of Ministry of Education, East China University of Science and Technology, Shanghai 200237, PR China^c Institute of Applied Chemistry, East China University of Science and Technology, Shanghai 200237, PR China

ARTICLE INFO

Article history:

Received 2 June 2012

Received in revised form

7 July 2012

Accepted 13 July 2012

Available online 23 July 2012

Keywords:

Pt–Pd nanoflakes

Screen-printed gold film electrode

Glucose

Nonenzymatic electrochemical sensor

ABSTRACT

The sluggish kinetic-controlled glucose oxidation reaction on Pt electrodes is well recognized as the most critical issue that blocks the development and commercialization of enzyme-free glucose sensors, and increasing attention is being focused on improving the analytical performances of these nonenzymatic sensors through exploring new Pt-based catalysts. In the present research, we synthesized novel Pt–Pd nanoflakes (Pt–Pd NFs) with three-dimensional architectures on a homemade screen-printed gold film electrode (SPGFE) substrate using a facile electrochemical deposition without any template, and further investigated the properties of the as-fabricated Pt–Pd NFs/SPGFE for enzymeless glucose detection. The results reveal that the proposed Pt–Pd nanostructure can provide preminent electrocatalytic activity and excellent selectivity for enzyme-free glucose sensing under simulative physiological conditions, mainly attributing to its attractive structure, large active surface and appropriate applied potential. The resulting Pt–Pd NFs/SPGFE offers linear current responses for glucose with the concentration upper limit to 16 mM. The obtained sensitivity is calculated to be as high as $48.0 \mu\text{A cm}^{-2} \text{mM}^{-1}$ in the presence of 0.15 M chlorides ions, and practical applications for blood sample analysis are also demonstrated. The proposed Pt–Pd structure is considered as a great potential building block for the fabrication of nonenzymatic electrochemical glucose sensors.

© 2012 Elsevier B.V. All rights reserved.

1. Introduction

Compared with enzyme electrodes, nonenzymatic glucose sensors based on the direct electrocatalytic oxidation of glucose exhibit several attractive advantages including sufficient stability, reproducibility of results, simplicity of operation and oxygen limitation-free. Pt-based materials such as various Pt nanostructures [1], mesoporous Pt surfaces [2], ordered Pt nanotubule arrays [3], macroporous Pt templates [4] and Pt/carbon composites [5] are recognized as promising building blocks for fabricating enzymeless electrochemical glucose sensors due to their outstanding catalytic activities. Although there have been few Pt structures used for the study of nonenzymatic continuous glucose monitoring in human blood [6], the sluggish glucose oxidation reaction on these Pt-based electrodes still hardly produces favorable faradaic responses to meet

commercial requirements for enzyme-free sensors. Therefore, intense research interest is continually focused on further facilitating the kinetic-controlled glucose electro-oxidation process to improve the poor sensitivity of nonenzymatic sensors [7–9]. Interestingly, modifying Pt surfaces with other metals to prepare Pt-based multi-metallic catalysts has been demonstrated capable of providing enhanced electrocatalytic performances for glucose sensing due to beneficial synergistic effects [10], and thus the synthesis of various Pt-based alloy structures and their applications in enzymeless glucose analysis have drawn increasing attention in recent years [11–13].

Herein, we introduce novel Pt–Pd nanoflakes (Pt–Pd NFs) with large active surfaces for nonenzymatic glucose sensing. The proposed structure was in situ synthesized on a homemade screen-printed gold film electrode (SPGFE) substrate using a facile electrodeposition. The electrochemical oxidation behavior of glucose in neutral media on the prepared Pt–Pd NFs was discussed. The overall analytical performance of the fabricated Pt–Pd NFs/SPGFE for enzyme-free glucose detection under simulative physiological conditions was also evaluated. As far as we know, up to now, there are very few reports about the electrochemical synthesis of Pt–Pd composites with analogous morphologies and

* Corresponding authors at: Shanghai Key Laboratory of Functional Materials Chemistry, and Research Centre of Analysis and Test, East China University of Science and Technology, Shanghai 200237, PR China. Tel.: +86 21 64253574; fax: +86 21 64252947.

E-mail addresses: minbolan@ecust.edu.cn (M. Lan), honglizhao@ecust.edu.cn (H. Zhao).

their applications in the fabrication of enzymeless sensors. Inspiringly, the resulting Pt–Pd NFs offer ultrahigh sensitivity for glucose determination in the presence of chloride ions.

2. Experimental

2.1. Synthesis and characterization of Pt–Pd NFs

The cathodic synthesis of Pt–Pd NFs was carried out on a CHI440A electrochemical workstation (CH Instruments), with a homemade SPGFE [14,15], a Pt wire and a 3 M KCl-saturated Ag/AgCl electrode as the working, counter and reference electrodes, respectively. In a typical synthesis, a clean SPGFE was immersed in a 0.1 M H₂SO₄ (Sinopharm Chemical Reagent Co.) solution containing 1 mM H₂PtCl₆·6H₂O (Sigma–Aldrich) and 1 mM PdCl₂ (Sinopharm Chemical Reagent Co.) for 5 min, followed by a cyclic voltammetric process from –0.6 to 0 V vs. Ag/AgCl for 15 segments at a scan rate of 5 mV/s; after deposition, the electrode was carefully rinsed with adequate ultrapure water (18.2 MΩ cm, Laboratory Water Purification System) and dried in air for further characterization and measurements. The surface morphology and elemental composition of the resulting Pt–Pd structure were characterized by field emission scanning electron microscopy (FESEM S-4800, Hitachi High-Technologies Co.) and energy-dispersive X-ray spectroscopy (EDS Falcon 60S, EDAX Inc.), respectively.

2.2. Electrochemical measurements

Cyclic voltammetric and chronoamperometric techniques were used to assess the electrocatalytic performance of the synthesized Pt–Pd NFs towards glucose (Sigma–Aldrich) oxidation in 0.1 M phosphate buffered solutions (PBS, pH = 7.4) with the absence or presence of chloride ions. All measurements were conducted on the aforementioned electrochemical workstation at room temperature (15 ± 2 °C), with solutions deoxygenated by bubbling highly pure argon before and during experiments. Amperometric responses were obtained after the transient steady states reached at the selected

potential with a constant stir (100 rpm). The geometric surface area of electrodes was used to calculate the current density.

3. Results and discussion

3.1. Synthesis and characterization of Pt–Pd NFs

In the present research, the Pt–Pd structure was in situ synthesized on the homemade SPGFE substrate using a simple electrodeposition process without templates. Compared with other synthesis methods including common sol–gel and hydrothermal approaches, electrochemically reducing precursors with controlled parameters is considered as a facile route to prepare nanomaterials. On the one hand, this method provides a convenient and environmental-friendly way to produce nanostructures without requirements of surfactants, high temperatures, organic solvents, etc.; on the other hand, materials are directly fabricated on desired electrode substrates, thus avoiding complicated modification steps. In addition, the size, shape, composition and microstructure of nanomaterials can be exquisitely adjusted by controlling electrochemical parameters.

The FESEM image, as shown in Fig. 1(A), demonstrates a scattered flake-like morphology of the synthesized material, which covers the whole gold film surface uniformly. The thickness of these flakes is determined to be approximately 7.4 nm. Furthermore, three-dimensional capacious architectures constructed by these nanoflakes with numerous crevices and holes are observed, which are supposed to be much beneficial for heterogeneous electrocatalysis due to their large surfaces and abundant active sites. Besides, these crevices and holes can fast mass transport of analytes through the electrode/electrolyte interface thanks to short diffusion length. To our best knowledge, there is still no report about the electrochemical synthesis of Pt–Pd bimetallic composites with similar structures. However, the detailed mechanism of forming this novel structure is unclear at present, and only a rough hypothesis may be made that the first positive-going segment produces numerous wire-like or network

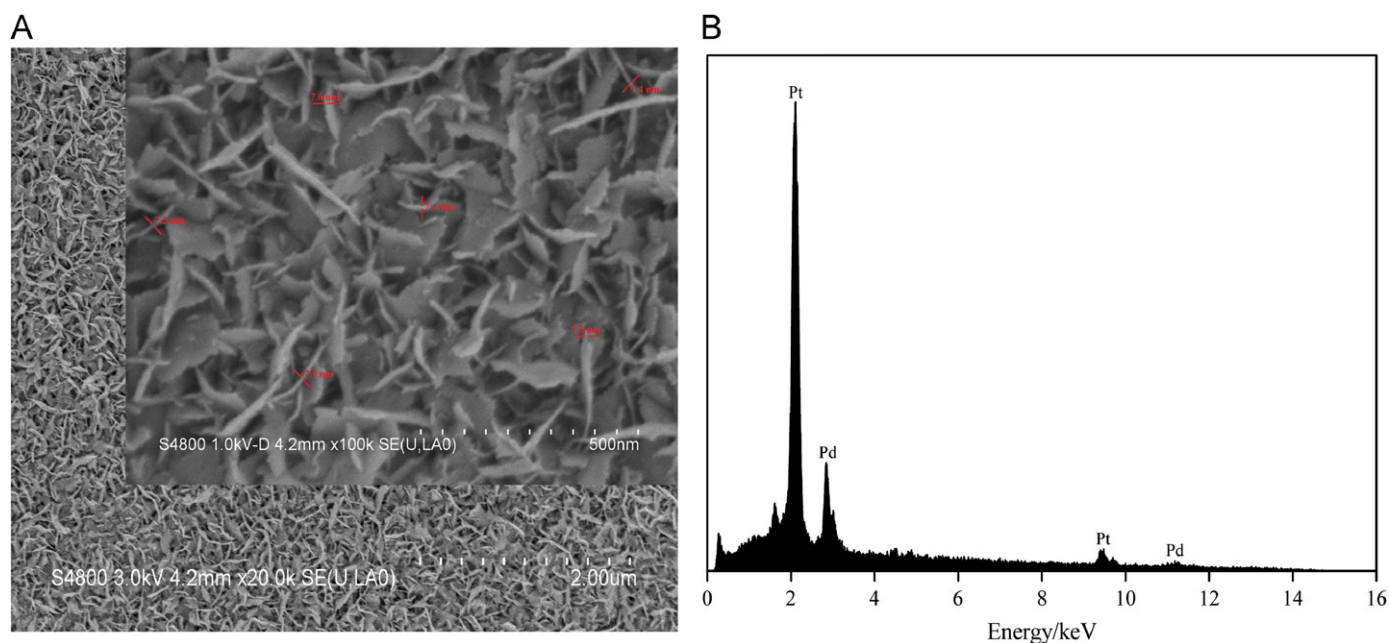


Fig. 1. (A) FESEM image of the synthesized Pt–Pd structure, and the inset shows the corresponding image with a higher magnification and (B) EDS pattern of the fabricated Pt–Pd NFs/SPGFE.

nucleuses, followed by a crystal growth process at such a low scan rate [16], and more work on clarifying the whole microcosmic procedure is much worthy for the further design and preparation of nanostructures with enhanced properties. The EDS pattern (Fig. 1(B)) displays the typical diffractions of Pt and Pd, revealing the successful synthesis of Pt–Pd alloy structures under proposed conditions. A quantitative EDS analysis by taking average values of reading at three different spots on the sample surface indicates that the Pt-based alloy with a Pd atomic proportion of 23% is obtained.

Fig. 2(A) depicts cyclic voltammograms of the bare SPGFE and Pt–Pd NFs/SPGFE in a 0.5 M H₂SO₄ solution at a scan rate of 10 mV/s. In the case of the bare SPGFE, a notable signal ascribed to the typical reduction of Au oxide is observed at around +0.9 V vs. Ag/AgCl. Differently, the resulting Pt–Pd NFs/SPGFE provides an overlapping reduction response of Pt and Pd oxides at +0.4 V, with the Au peak reduced seriously. Moreover, two pairs of reversible peaks are observed at approximately –0.15 and 0 V, corresponding to the hydrogen adsorption/desorption responses on the Pt-based electrode surface [11]. Although the active surface area of the Pt–Pd NFs/SPGFE cannot be precisely determined by integrating the charge required for hydrogen adsorption with metal loading simply [17], on the basis of the observed FESEM image (Fig. 1(A)), the prepared Pt–Pd NFs expose a large surface. In addition, the results of cyclic voltammograms in the ferricyanide system (a solution composed of 2 mM K₃[Fe(CN)₆] and 0.5 M KCl), as illustrated in Fig. 2(B), demonstrate that the proposed Pt–Pd NFs/SPGFE can exhibit slightly better performance for promoting electron transfer on the electrode/electrolyte interface in comparison with the bare SPGFE, because the peak potential difference (ΔE_p) for the Pt–Pd NFs/SPGFE (91 mV) is found to be smaller than that for the SPGFE (102 mV) [18]. Moreover, the calculated peak current (I_p) on the Pt–Pd NFs/SPGFE is also slightly larger.

3.2. Glucose sensing on Pt–Pd NFs/SPGFE

3.2.1. Electrocatalytic activity towards glucose oxidation

The electrocatalytic activity of the proposed Pt–Pd NFs was evaluated by investigating the electrochemical behavior of glucose in neutral media. Fig. 3 presents cyclic voltammograms of the bare SPGFE and Pt–Pd NFs/SPGFE in 0.1 M PBS (pH = 7.4) with the

absence or presence of 10 mM glucose at a scan rate of 10 mV/s. In respect of the SPGFE, much similar responses between the absence and the presence of glucose are observed in the selected potential window, with no notable signal of glucose electro-oxidation obtained. This phenomenon indicates that the bare SPGFE substrate exhibits negligible electrocatalytic activity towards glucose oxidation due to the intrinsic poor activity of Au [19] and its mirror-like surface [20]. As for the fabricated Pt–Pd NFs/SPGFE, a remarkable peak (I) attributed to the initial adsorption and oxidation of glucose on the Pt-based electrode surface is observed at approximately –0.3 V vs. Ag/AgCl, followed by a shoulder at –0.15 V (II) and a small signal at +0.17 V (III) for the further oxidation of intermediates. When scanning the potential towards more positive values, Pt and Pd start to be electrochemically oxidized, with a broad response (IV) starting from +0.4 V in PBS. Correspondingly, the reduction peak (V) of Pt and Pd oxides appears at around 0 V.

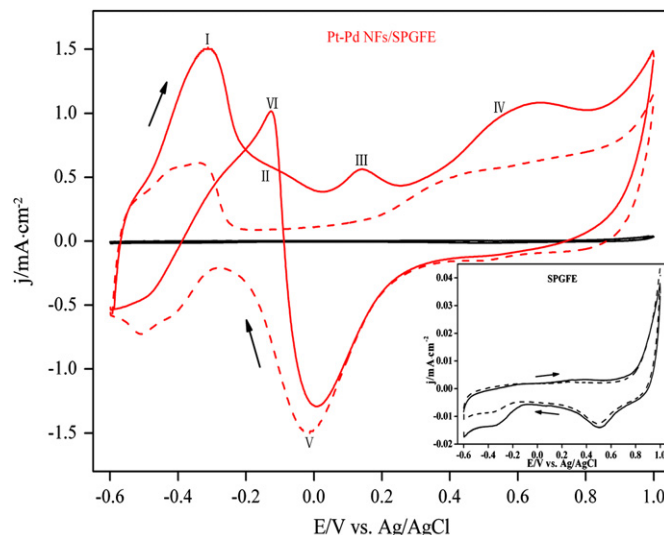


Fig. 3. Cyclic voltammograms of the bare SPGFE (in black) and Pt–Pd NFs/SPGFE (in red) in 0.1 M PBS (pH = 7.4) with the absence (dotted curves) or presence (solid curves) of 10 mM glucose at a scan rate of 10 mV/s, and the inset presents the magnified cyclic voltammograms of the bare SPGFE. (For interpretation of the references to color in this figure caption, the reader is referred to the web version of this article.)

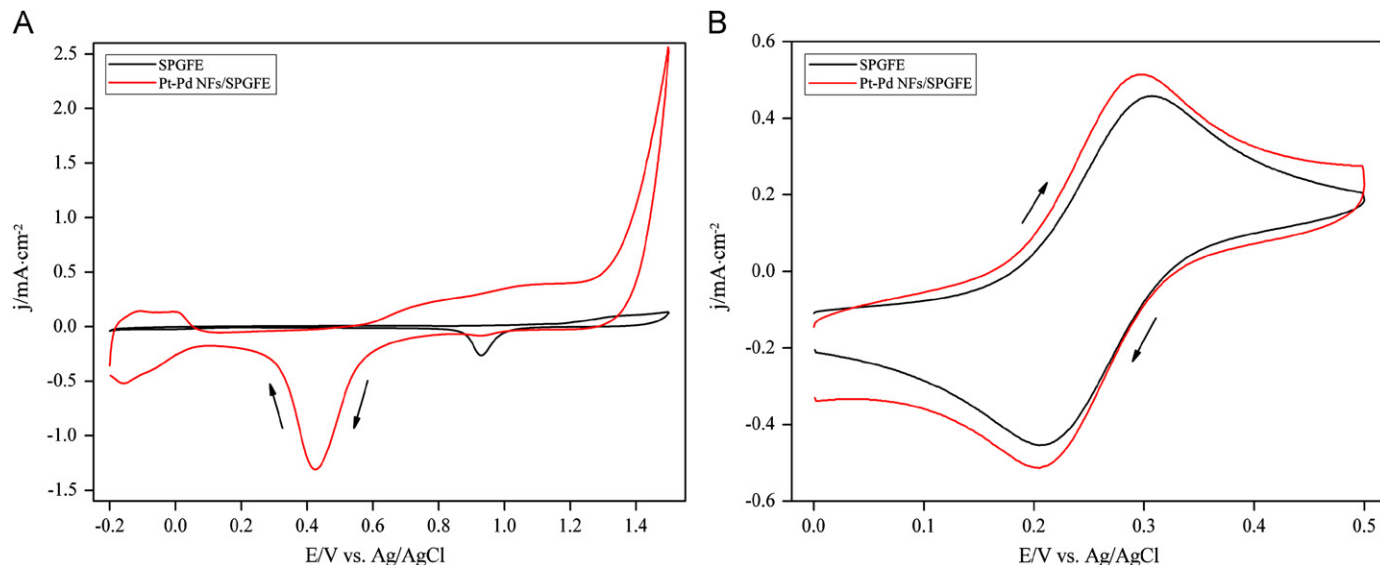


Fig. 2. (A) Cyclic voltammograms of the bare SPGFE and Pt–Pd NFs/SPGFE in a 0.5 M H₂SO₄ solution at a scan rate of 10 mV/s and (B) cyclic voltammograms of the bare SPGFE and Pt–Pd NFs/SPGFE in a 2 mM K₃[Fe(CN)₆] solution containing 0.5 M KCl at a scan rate of 50 mV/s.

Importantly, glucose produces the typical behavior (VI) of electrochemical oxidation in the ‘hydrogen region’ [21], which is unique only when Pt-based materials are used as the working electrode [22]. Compared to well recognized nanoporous Pt [2] and Pt–Pb [11] materials, the synthesized Pt–Pd structure presents higher electrocatalytic activity (as high as $0.151 \text{ mA cm}^{-2} \text{ mM}^{-1}$) towards glucose oxidation under identical conditions based on the response at -0.3 V (I), mainly attributing to its large active surface and unique nanostructure.

3.2.2. Poisoning resistance upon chloride ions

The activity of Pt is usually impaired by adsorbed chloride ions and intermediates that originate from glucose electro-oxidation, which is known as a critical issue for Pt-based nonenzymatic glucose sensors [11]. We also tested the poisoning resistance of the synthesized Pt–Pd NFs upon chloride ions. Fig. 4(A) depicts positive-going portions of cyclic voltammograms of the fabricated Pt–Pd NFs/SPGFE in 0.1 M PBS (pH = 7.4) containing 10 mM glucose with the absence or presence of chloride ions. In the presence of 0.15 M KCl, glucose provides similar oxidation behaviors to that without chloride ions. However, faradaic currents are considerably reduced when chloride ions are added, and a 63.3% current density on the basis of the signal at -0.3 V is retained. This phenomenon can be explained by that the adsorbed chloride ions cover the catalytic surface and block active sites [23]. Therefore, a research on enhancing the poisoning resistance capability of the Pt-based catalyst is under processing, based on an interesting report involving the stabilization of Pt oxygen-reduction electro-catalysts with gold clusters [24].

3.2.3. Selectivity

Commonly, other physiological species including ascorbic acid (AA), 4-acetamidophenol (AP) and uric acid (UA) may be oxidized and produce interfering responses for glucose sensing. The selectivity of the fabricated Pt–Pd NFs/SPGFE for amperometric glucose determination at an applied potential of -0.3 V vs. Ag/AgCl was assessed in this study. As illustrated in Fig. 4(B), it demonstrates that the addition of AA and UA hardly provides notable interference for glucose sensing, and 0.1 mM AP only makes a poor increase of currents, indicating that the proposed electrode can be employed to detect glucose selectively. This favorable selectivity

is ascribed to the much negative applied potential (-0.3 V vs. Ag/AgCl), where these species cannot be oxidized. Wang et al. also found that glucose sensing on a nanoporous Pt–Pb modified electrode at a potential of -0.08 V vs. Ag/AgCl would not be interfered by these common species in blood [11]. As a matter of fact, we demonstrate that these species start to be oxidized only when the applied potential positively reaches to $+0.2 \text{ V}$ vs. Ag/AgCl (data not shown).

3.2.4. Overall performance for nonenzymatic glucose sensing

Finally, we evaluated the overall performance of the proposed Pt–Pd NFs/SPGFE for nonenzymatic glucose sensing in neutral media. Fig. 5(A) presents chronoamperometric curves of the fabricated Pt–Pd NFs/SPGFE in 0.1 M PBS (pH = 7.4) containing 0.15 M chloride ions upon successive addition of 1 mM glucose at -0.3 V vs. Ag/AgCl. Although the aforementioned reduction of electrocatalytic activity induced by chloride ions, the results reveal that the Pt–Pd NFs/SPGFE still can be used to detect glucose under simulated physiological conditions, providing linear current responses upon the concentration of glucose up to 16 mM with a linear equation of $j \text{ (mA cm}^{-2}\text{)} = 0.04801C \text{ (mM)} + 0.01601$ and a correlation coefficient (R^2) of 0.9991. This wide linear scope completely covers the normal physiological level of glucose (3–8 mM) in human blood. The sensitivity is further calculated to be as high as $48.0 \mu\text{A cm}^{-2} \text{ mM}^{-1}$. Compared with those well-known catalysts used for nonenzymatic glucose sensing, as listed in Table 1, the sensitivity obtained on the Pt–Pd NFs is very attractive. This ultrahigh sensitivity is supposed to be mainly ascribed to the unique nanostructure and large active surface. The limit of detection (LOD) is determined to be $20.6 \mu\text{M}$ based on a signal to noise of 3 ($S/N = 3$). In addition, a set of eight amperometric measurements for 5 mM glucose at a single Pt–Pd NFs/SPGFE result in a relative standard deviation (RSD) of 2.1%, revealing an excellent repeatability of these measurements. Eight electrodes prepared under proposed conditions are used to test the reliability of the synthesis method, and a RSD of 4.3% is obtained for detecting 5 mM glucose, indicating that the resulting electrodes exhibit very similar electrocatalytic properties for glucose oxidation. Besides, FESEM images from three fabricated electrodes also demonstrate the same flake-like morphology. When not in use, these fabricated sensors are stored in air, and over 96% of electrocatalytic activity is obtained after seven

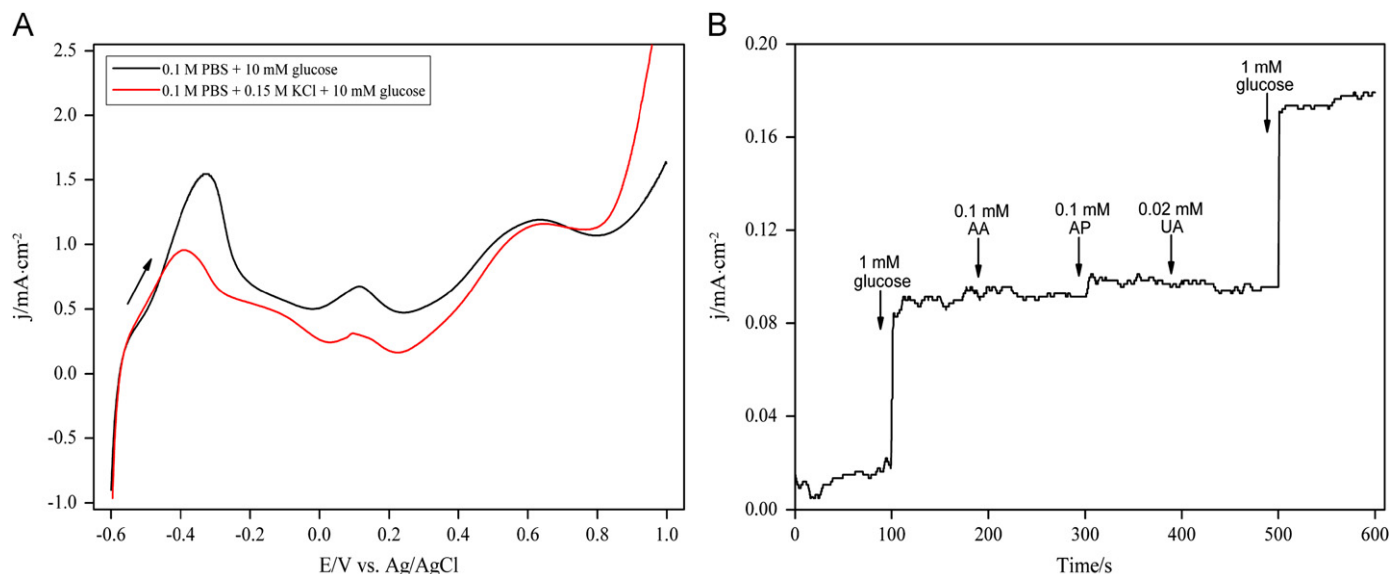


Fig. 4. (A) Positive-going portions of cyclic voltammograms of the fabricated Pt–Pd NFs/SPGFE in 0.1 M PBS (pH = 7.4) containing 10 mM glucose with the absence or presence of 0.15 M KCl at a scan rate of 10 mV/s and (B) chronoamperometric responses of the Pt–Pd NFs/SPGFE in 0.1 M PBS (pH = 7.4) upon successive addition of 1 mM glucose, 0.1 mM AA, 0.1 mM AP, 0.02 mM UA and 1 mM glucose at an applied potential of -0.3 V vs. Ag/AgCl.

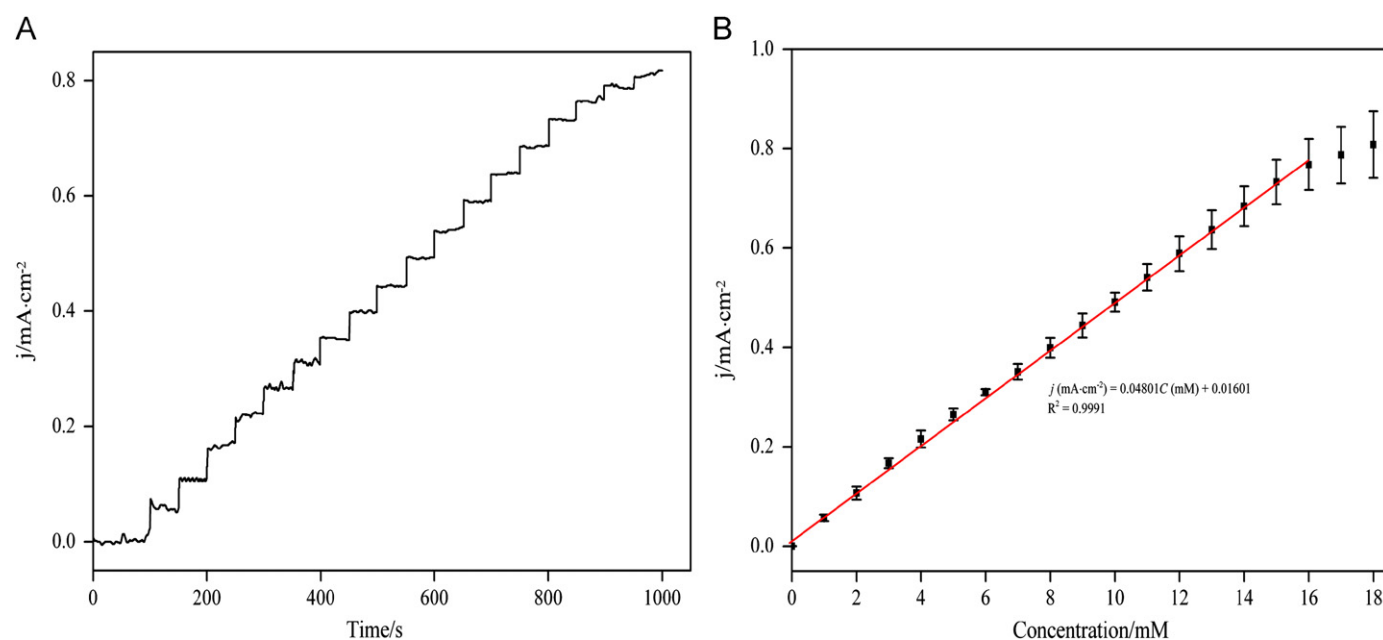


Fig. 5. (A) Chronoamperometric responses of the Pt–Pd NFs/SPGFE in 0.1 M PBS (pH = 7.4) containing 0.15 M KCl upon successive addition of 1 mM glucose at -0.3 V vs. Ag/AgCl and (B) relationships between obtained steady-state currents and glucose concentrations ($n = 3$).

Table 1

Comparisons of the linear range and sensitivity between the proposed Pt–Pd nanoflakes and typical materials used for nonenzymatic glucose sensing in neutral media.

Material	Linear range (mM)	Sensitivity ($\mu\text{A cm}^{-2} \text{mM}^{-1}$)	Reference
Mesoporous Pt	0–10	9.6	[2]
Ordered Pt nanotubule arrays	2–14	0.1	[3]
Nanoporous Pt–Pb networks	1–16	10.8	[11]
3D ordered macroporous Pt template	0.001–10	31.3	[4]
Pt–Pb nanowire arrays	0–11	11.25	[12]
Gold nanotube arrays	1–42.5	1.13	[25]
3D coral-like macroporous Au–Pt	0–20	39.53	[19]
Self-supported porous Au	2–10	11.8	[26]
Pt nanoflower-SWCNT membrane	0.002–10	7.266	[5]
Urchin-like gold sub-microstructure	0.2–13.2	16.8	[27]
Pt–Pd NFs	0–16	48.0	This work

Table 2

Comparisons of the results for blood sample analysis obtained by the commercial glucometer and the proposed Pt–Pd NFs/SPGFE enzymeless sensor.

Sample	Commercial glucometer (mM) ($n = 3$)	Proposed Pt–Pd NFs/SPGFE (mM) ($n = 3$)
1#	7.7	7.73 ± 0.16
2#	6.7	6.77 ± 0.13
3#	5.6	5.71 ± 0.12

days. This good stability is mainly ascribed to the fact that no biological species (e.g., GO_x) is employed in comparison with enzyme electrodes.

In order to verify the potential applications of the proposed sensor in practical analysis, we further utilized the fabricated Pt–Pd NFs/SPGFE to detect glucose in blood samples from ICR

mice, and a commercial One-Touch Ultra glucometer (Johnson & Johnson Medical Ltd.) was used as a reference tool. Consistent results are obtained for the two sensors, as shown in Table 2, demonstrating that the fabricated Pt–Pd NFs/SPGFE can be utilized in practical sample analysis accurately.

4. Conclusions

In summary, novel Pt–Pd nanoflakes with large active surfaces have been successfully synthesized on the screen-printed gold film substrate using a facile electrodeposition. The fabricated Pt–Pd NFs/SPGFE exhibits very attractive electrocatalytic activity towards glucose oxidation in neutral media. Excellent selectivity for nonenzymatic glucose sensing is also demonstrated. Although partly poisoned by chloride ions, this new Pt–Pd catalyst with three-dimensional nanoflake architectures presents favorable overall performance for enzymeless glucose detecting under simulated physiological conditions, and is a great promising candidate for the fabrication of enzyme-free glucose monitoring devices for practical analysis.

Acknowledgments

Research grants from Science and Technology Commission of Shanghai Municipality (nos. 10dz2220500 and 10391901600) and Ministry of Education of the People's Republic of China (no. WK1014051) are gratefully acknowledged.

References

- [1] S.J. Guo, E.K. Wang, *Nano Today* 6 (2011) 240–264.
- [2] S. Park, T.D. Chung, H.C. Kim, *Anal. Chem.* 75 (2003) 3046–3049.
- [3] J.H. Yuan, K. Wang, X.H. Xia, *Adv. Funct. Mater.* 15 (2005) 803–809.
- [4] Y.Y. Song, D. Zhang, W. Gao, X.H. Xia, *Chem. Eur. J.* 11 (2005) 2177–2182.
- [5] L. Su, W.Z. Jia, L.C. Zhang, C. Beacham, H. Zhang, Y. Lei, *J. Phys. Chem. C* 114 (2010) 18121–18125.
- [6] S. Park, S. Park, R.A. Jeong, H. Boo, J. Park, H.C. Kim, T.D. Chung, *Biosens. Bioelectron.* 31 (2012) 284–291.
- [7] Y. Myung, D.M. Jang, Y.J. Cho, H.S. Kim, J. Park, J.U. Kim, Y. Choi, C.J. Lee, *J. Phys. Chem. C* 113 (2009) 1251–1259.

- [8] D. Rathod, C. Dickinson, D. Egan, E. Dempsey, *Sens. Actuators B* 143 (2010) 547–554.
- [9] Y.Y. Song, Z.D. Gao, K. Lee, P. Schmuki, *Electrochem. Commun.* 13 (2011) 1217–1220.
- [10] Y.P. Sun, H. Buck, T.E. Mallouk, *Anal. Chem.* 73 (2001) 1599–1604.
- [11] J.P. Wang, D.F. Thomas, A.C. Chen, *Anal. Chem.* 80 (2008) 997–1004.
- [12] Y. Bai, Y.Y. Sun, C.Q. Sun, *Biosens. Bioelectron.* 24 (2008) 579–585.
- [13] F.Q. Zhao, F. Xiao, B.Z. Zeng, *Electrochem. Commun.* 12 (2010) 168–171.
- [14] Y.J. Teng, S.H. Zuo, M.B. Lan, *Biosens. Bioelectron.* 24 (2009) 1353–1357.
- [15] X.H. Niu, Y.L. Ding, C. Chen, H.L. Zhao, M.B. Lan, *Sens. Actuators B* 158 (2011) 383–387.
- [16] B. Lim, Y.N. Xia, *Angew. Chem. Int. Ed.* 50 (2011) 76–85.
- [17] I.E.L. Stephens, A.S. Bondarenko, U. Gronbjerg, J. Rossmeisl, I. Chorkendorff, *Energy Environ. Sci.* 5 (2012) 6744–6762.
- [18] H.C. Wang, X.S. Wang, X.Q. Zhang, X. Qin, Z.X. Zhao, Z.Y. Miao, N. Huang, Q. Chen, *Biosens. Bioelectron.* 25 (2009) 142–146.
- [19] Y.J. Lee, J.Y. Park, *Sens. Actuators B* 155 (2011) 134–139.
- [20] X.H. Niu, H.L. Zhao, C. Chen, M.B. Lan, *Electrochim. Acta* 65 (2012) 97–103.
- [21] S. Ernst, J. Heitbaum, C.H. Hamann, *J. Electroanal. Chem.* 100 (1979) 173–177.
- [22] S. Park, H. Boo, T.D. Chung, *Anal. Chim. Acta* 556 (2006) 46–57.
- [23] A. Lam, H. Li, S.S. Zhang, H.J. Huang, D.P. Wilkinson, S. Wessel, T.T.H. Cheng, *J. Power Sources* 205 (2012) 235–238.
- [24] J. Zhang, K. Sasaki, E. Sutter, R.R. Adzic, *Science* 315 (2007) 220–222.
- [25] Y.G. Zhou, S. Yang, Q.Y. Qian, X.H. Xia, *Electrochem. Commun.* 11 (2009) 216–219.
- [26] Y. Li, Y.Y. Song, C. Yang, X.H. Xia, *Electrochem. Commun.* 9 (2007) 981–988.
- [27] F.G. Xu, K. Cui, Y.J. Sun, C.L. Guo, Z.L. Liu, Y. Zhang, Y. Shi, Z. Li, *Talanta* 82 (2010) 1845–1852.